

One-particle interchain hopping in coupled Hubbard chains

D. Poilblanc¹, H. Endres², F. Mila¹, M. G. Zacher², S. Capponi¹ and W. Hanke²

¹Laboratoire de Physique Quantique, Université Paul Sabatier, 31062 Toulouse, France

²Institute for Physics, University of Wurzburg, D-97074 Wurzburg, Germany

(October 95)

Interchain hopping in systems of coupled chains of correlated electrons is investigated by exact diagonalizations and Quantum-Monte-Carlo methods. For two weakly coupled Hubbard chains at commensurate densities (e.g. $n=1/3$) the splitting at the Fermi level between bonding and antibonding bands is strongly reduced (but not suppressed) by repulsive interactions extending to a few lattice spacings. The magnitude of this reduction is directly connected to the exponent α of the 1D Luttinger liquid. However, we show that the incoherent part of the single particle spectral function is much less affected by the interchain coupling. This suggests that incoherent interchain hopping could occur for intermediate α values.

PACS Numbers: 71.27.+a, 71.38.+i, 74.20.Mn, 74.25.Kc

The possible occurrence of incoherent single-particle hopping in strongly correlated systems is presently actively debated. Such an unusual behavior could, for example, explain the unconventional c-axis conductivity found in two-layered high- T_c compounds [1]. In addition, the high transition temperatures of these materials may also be connected to incoherent hopping [2]: as a consequence of incoherence, the coupled planes can lower the total energy by coherent pair-hopping processes, leading to an amplification of the tendency towards superconducting pairing.

Perturbation and renormalisation-group treatments [3–5] of the transverse hopping between chains reveals that the key parameter which governs interchain hopping is the non-universal exponent α of the 1D Luttinger liquid (LL) [6] characterizing the low frequency behavior of the density of state $N(\omega) \sim \omega^\alpha$. For $\alpha \geq 1$, ie for sufficiently strong interaction, the interchain hopping becomes irrelevant. Recently Clarke, Strong and Anderson [7] suggested a somewhat different criterium: let us consider, for (real) times $\tau < 0$, a system of two decoupled chains with different electron numbers on each chain in some initial state $|\Psi_0\rangle$. Then, if the interchain hopping t_\perp is switched on at $\tau = 0$ two different behaviors can be observed: the quantity $P(\tau) = |A(\tau)|^2$, with $A(\tau) = \langle \Psi_0 | e^{iH\tau} | \Psi_0 \rangle$ corresponding to the probability for the system to be in its initial state, at a later time $\tau > 0$ might show oscillatory or monotoneous behaviors characterizing “coherent” or “incoherent” interchain hopping, respectively. It was suggested that such an incoherent behavior could occur at values of α as small as 0.5.

The first numerical attempt to examine the question of coherent versus incoherent single particle hopping was initiated by two of us [8]. By exact diagonalizations of two coupled t-J chains, an interesting connection between coherence and integrability was found. However, it should be emphasized that, in this approach, the initial state $|\Psi_0\rangle$ at $\tau = 0$ is far from equilibrium. Indeed, con-

structing the whole system with $t_\perp = 0$ corresponds to a macroscopic perturbation for the full hamiltonian (including the transverse hopping). Interchain *single* particle hopping in the true GS ($t_\perp \neq 0$) is still an open question.

For this purpose, let us first consider two weakly coupled chains described by an extended Hubbard model,

$$H = -t \sum_{i,\lambda,\sigma} (c_{i,\lambda,\sigma}^\dagger c_{i+1,\lambda,\sigma} + h.c.) + U \sum_{i,\lambda} n_{i,\lambda,\uparrow} n_{i,\lambda,\downarrow} + \sum_{r,i,\lambda} V_r n_{i,\lambda} n_{i+r,\lambda} - t_\perp \sum_{i,\lambda,\sigma} (c_{i,1,\sigma}^\dagger c_{i,2,\sigma} + h.c.), \quad (1)$$

where $c_{i,\lambda,\sigma}^\dagger$ is a creation fermion operator at site i of the chain λ ($=1,2$). We shall deal here with two cases; (i) a purely on-site interaction ($V_r = 0$) or (ii) an extended repulsion of the form $V_r = U/(r+1)$ limited to $r=1$ and 2.

In contrast to previous numerical work, we shall assume that, at $\tau < 0$, the system contains M electrons in the ground state (GS) $|\phi_0\rangle$ of the full hamiltonian (1) and that, at $\tau = 0$, only a *single* extra particle (e.g. a hole) of longitudinal momentum k is added to, let say, chain number 1. Provided the occupation number $n_{k,1} = \langle \phi_0 | c_{k,1,\sigma}^\dagger c_{k,1,\sigma} | \phi_0 \rangle$ is non zero, the corresponding probability $P(\tau)$ is then defined by the amplitude $A(\tau) = \int_{-\infty}^{\infty} A(\omega) e^{i\omega\tau} d\tau / n_{k,1}$, with

$$A(\omega) = -\frac{1}{\pi} \text{Im} \left\{ \langle \phi_0 | c_{k,1,\sigma}^\dagger \frac{1}{\omega + i\epsilon - H + E_0^M} c_{k,1,\sigma} | \phi_0 \rangle \right\}. \quad (2)$$

This corresponds to the particular choice of an initial (normalized) state of the form $|\Psi_0\rangle = \frac{1}{(n_{k,1})^{1/2}} c_{k,1,\sigma} | \phi_0 \rangle$. Note that when an electron is added instead of a hole the creation and annihilation operators in (2) have to be interchanged. At finite temperature $T = 1/\beta$ all expectation values in $|\phi_0\rangle$ must be replaced by thermal averages.

Writing $c_{k,1,\sigma}$ in terms of the bonding and anti-bonding operators $c_{k,k_\perp,\sigma}$ ($k_\perp = 0, \pi$) it is straightforward to

express (2) as a linear combination, $A(\omega) = (A(k, 0, \omega) + A(k, \pi, \omega))/(1 + e^{\beta(\omega - \mu)})$ where $A(\mathbf{k}, \omega) = -\frac{1}{\pi} \text{Im} G(\mathbf{k}, \omega)$ corresponds to the usual spectral function in momentum space ($\mathbf{k} = (k, k_{\perp})$). At this point, it is instructive to consider the non-interacting $U=0$ limit (and $T = 0$). In this case, $A(\mathbf{k}, \omega) \sim \delta(\omega - \epsilon_{\mathbf{k}})$ and the two bands $\epsilon_{\mathbf{k}}$ for $k_{\perp} = 0$ and π are split by $2t_{\perp}$. If the momentum \mathbf{k} (close to k_F) is chosen in such a way that both $k_{\perp} = 0$ and $k_{\perp} = \pi$ states in $|\phi_0\rangle$ are occupied, $P(\tau)$ acquires an oscillatory behavior with a characteristic time scale π/t_{\perp} .

For a generic LL the quasiparticle δ -peak is in fact replaced by a singularity [9] corresponding to a collective excitation (in fact split holon and spinon peaks). However, it is clear that an oscillatory behavior of $P(\tau)$ is only possible if t_{\perp} splits the dispersion relation of the bonding and anti-bonding modes by a finite amount although this alone might not be sufficient. One possible scenario would be that the whole spectra for $k_{\perp} = 0$ or π (i.e. the poles of the one particle Green functions) would be displaced by $\pm t_{\perp}$ respectively. In this case, $P(\tau)$ would exactly take the form $\cos^2(t_{\perp}\tau)P_{1D}(\tau)$ where $P_{1D}(\tau)$ is independent of t_{\perp} and is directly related to the 1D spectral function $A_{1D}(k, \omega)$ of the LL. However, we expect that, in general, (i) the incoherent part of $A_{1D}(k, \omega)$ (i.e the part not related to the collective mode) is less sensitive to the transverse hopping at energies $\omega \gg t_{\perp}$ and (ii) the relative weight of this part increases with the strength and the range of the interaction within the chains. Since analytic approaches of such a problem are extremely difficult, we shall rely in the following on exact diagonalizations of finite clusters (where dynamical and time dependent quantities can be calculated exactly) and on Quantum Monte Carlo (QMC) data.

As a preliminary study, the various LL parameters of the 1D *single chain* (e.g. α , K_{ρ} , spin and charge velocities, etc...) are determined. The parameters of the 1D on-site Hubbard model are known from numerical calculations based on the Bethe Ansatz [10]. In the case of the extended model these parameters are obtained by standard finite-size scaling of ED results. For more technical details the reader can refer to Ref. [11]. Hereafter, we shall restrict ourselves to a fermion density of $n=1/3$ where relatively large values of the exponent α (up to ~ 1.78) can in principal be obtained [12]. Our numerical data show that the maximum value can be realized in the case of the extended model for $U \sim 10.5$. Above this value a gap appears in the single particle spectral density possibly signaling a metal-insulator transition of no interest for us in the present work.

The result for the spectral function of the double Hubbard chain deduced by analytic continuation of the QMC data by maximum entropy methods is shown in Fig. (1) for $U/t = 8$. Bonding and anti-bonding bands dispersing through the fermi level ($\omega = \mu = 0$) can be clearly seen. Although error bars are rather large [13] a splitting ΔE of order $2t_{\perp}$ can be measured. It is *a priori* puzzling that such a large U does not lead to a substantial reduction of

the splitting. However, one has to remember that α remains very small for an on-site interaction, e.g. $\alpha \sim 0.07$ for $U/t = 8$.

As a comparison, the dispersions of the two low-energy branches corresponding to sharp peaks in $A(\mathbf{k}, \omega)$ for $k_{\perp} = 0$ and $k_{\perp} = \pi$ and obtained by ED techniques are shown in Fig. (2) for the same value of U , in qualitative agreement with the QMC results. Note that the boundary conditions along the chain direction (periodic or anti-periodic) are always chosen in such a way that the GS $|\phi_0\rangle$ has a closed shell configuration. It should be emphasized that the band splitting picture is only valid sufficiently close to the Fermi level μ and that, on finite clusters, different values are obtained immediately above (i.e. $|k| > k_F$) or below (i.e $|k| < k_F$) the chemical potential μ .

A careful study of the ED data reveals that ΔE , for sufficiently small t_{\perp} , behaves like $at_{\perp} + bt_{\perp}^3$, where a and b depend on the parameters and system size. The ratio in the limit of vanishing t_{\perp} is then easily extracted and the results are displayed in Fig. (3a) for the Hubbard and the extended Hubbard models and various system size. Assuming finite size corrections of the form $1/L_x$ [14], where L_x is the length of the chains, and considering the average between the splittings above and below μ , one can also estimate $\Delta E/2t_{\perp}$ in the thermodynamic limit as seen in Fig. (3b). Clearly repulsion at intermediate distances is much more effective to reduce the splitting. However, the plot of the same data vs α instead of U in (3b) suggests that α alone seems to be the key parameter controlling the splitting. Indeed, an extended interaction leads to larger α values and hence to smaller $\Delta E/2t_{\perp}$.

The previous study suggests that, at least for $\alpha < 1$, a transverse hopping t_{\perp} leads to a splitting of the bonding and anti-bonding branches in agreement with perturbative treatments of t_{\perp} [3–5]. However, the expression for $P(\tau)$ involves the whole spectral function $A(\mathbf{k}, \omega)$ at all frequencies so that it is not clear whether a splitting of the low energy singularity alone will necessarily lead to a coherent interchain behavior. The spectral functions at $k_{\perp} = 0$ and $k_{\perp} = \pi$ of the on-site Hubbard model and for a momentum \mathbf{k} close to k_F are shown in Fig. (4a). Most of the spectral weight is located at the low energy singularity which is clearly split by the transverse hopping t_{\perp} . On the contrary, in the case of the extended Hubbard model (with parameters such that $\alpha \sim 0.53$) shown in Fig. (4b), more spectral weight appears far from the Fermi level and is less affected by t_{\perp} .

The probability $P(\tau)$ has been computed from the knowledge of the spectral functions shown in Figs. (4a,b) and results are shown in Fig. (5). For the two types of models we observe both fast and slow oscillations which have different physical origins. The fast oscillations are due to the fine structure of the 1D spectral function $A_{1D}(\mathbf{k}, \omega)$ (i.e. for $t_{\perp} = 0$); for example, the sharp peaks of Fig. (4b) might be attributed to shadow bands [15]. We expect that, in the thermodynamic limit, these peaks will broaden and hence the fast oscillations will

get strongly damped if not suppressed. More interestingly, the slow oscillations have a pseudo-periodicity of order $\pi/\Delta E$ and are due to the effect of t_{\perp} . They reveal some degree of interchain coherence. However, in the case of the extended Hubbard model with $\alpha \sim 0.53$ a larger damping can be seen. It is not clear yet whether these slow oscillations will completely disappear in the thermodynamic limit.

The previous results suggest that a splitting of the dispersion of the single-particle low-energy mode of the LL by the transverse coupling alone does not necessarily lead to an oscillatory behavior of $P(\tau)$ which, according to Ref. [7], characterizes a coherent interchain hopping. Indeed, for a sufficiently repulsive intermediate range (e.g. up to distances of 2 or 3 lattice spacings) interaction the large incoherent part of the single-particle 1D spectral function might play a very important role in preventing coherent interchain hopping.

DP acknowledges support from the EEC Human Capital and Mobility program under Grant No. CHRX-CT930332. WH acknowledges EC Grant No. ERBCHRX-CT940438 and the Bavarian FORSUPRA Program. We also thank IDRIS, Orsay (France), for allocation of CPU time on the C94 and C98 CRAY supercomputers, and the HLRZ Jülich and LRZ München for access to the CRAY Y-MP supercomputers.

-
- [1] S.L. Cooper et al., Phys. Rev. Lett. **70**, 1533 (1993); Y. Maeno et al., Nature **372**, 532 (1994).
[2] P. W. Anderson, Phys. Rev. Lett. **67**, 3844 (1991).
[3] H. J. Schulz, Int. J. Mod. Phys. B **5**, 57 (1991).
[4] M. Fabrizio, A. Parola and E. Tosatti, Phys. Rev. B **46** 3159 (1992); C. Castellani, C. di Castro and W. Metzner, Phys. Rev. Lett. **69**, 1703 (1992); M. Fabrizio, Phys. Rev. B **48**, 15838 (1993).
[5] C. Bourbonnais and L. G. Caron, Int. J. Mod. Phys. B **5**, 11033 (1991); D. Boies, C. Bourbonnais, and A.-M.S. Tremblay, Phys. Rev. Lett. **74**, 968 (1995).
[6] F. D. M. Haldane, J. Phys. C **14**, 2585 (1981); see also J. Sólyom, Adv. Phys. **28**, 209 (1979).
[7] D. G. Clarke, S. P. Strong and P. W. Anderson, Phys. Rev. Lett. **72**, 3218 (1994); see also S. Chakravarty, A. Sudbø, P. W. Anderson and S. P. Strong, Science **261**, 337 (1993); D. G. Clarke and S. P. Strong, Sissa/cond-mat9510168 preprint (1995).
[8] F. Mila and D. Poilblanc, Phys. Rev. Lett. **76**, 287 (1996).
[9] V. Meden and K. Schönhammer, Phys. Rev. B **46**, 15753 (1992); J. Voit, Phys. Rev. B **47**, 6740 (1993); K. Penc, F. Mila and H. Shiba, Sissa/cond-mat9501085 preprint (1995).
[10] H. J. Schulz, Phys. Rev. Lett. **64** 2831, (1990).
[11] F. Mila and X. Zotos, Europhys. Lett. **24**, 133 (1993).
[12] H. J. Schulz, “Correlated Electron Systems”, p. 199, ed.

V. J. Emery (World Scientific, Singapore, 1993); H. J. Schulz, “Strongly Correlated Electronic Materials: The Los Alamos Symposium 1993”, p. 187, ed. K. S. Bedell, Z. Wang, D. E. Meltzer, A. V. Balatsky, E. Abrahams (Addison-Wesley, Reading, Massachusetts, 1994).

- [13] More accurate determination of the splitting from QMC can be obtained from the relative shift of the occupation numbers $n_{\mathbf{k}}$ for $k_{\perp} = 0$ and $k_{\perp} = \pi$. See H. Endres et al. (in preparation).
[14] $1/L_x$ finite size corrections are in fact clearly established in the case of coupled spinless fermion chains; See S. Capponi et al. (in preparation).
[15] K. Penc, K. Hallberg, F. Mila and H. Shiba, Sissa/cond-mat9512152 preprint (1995).

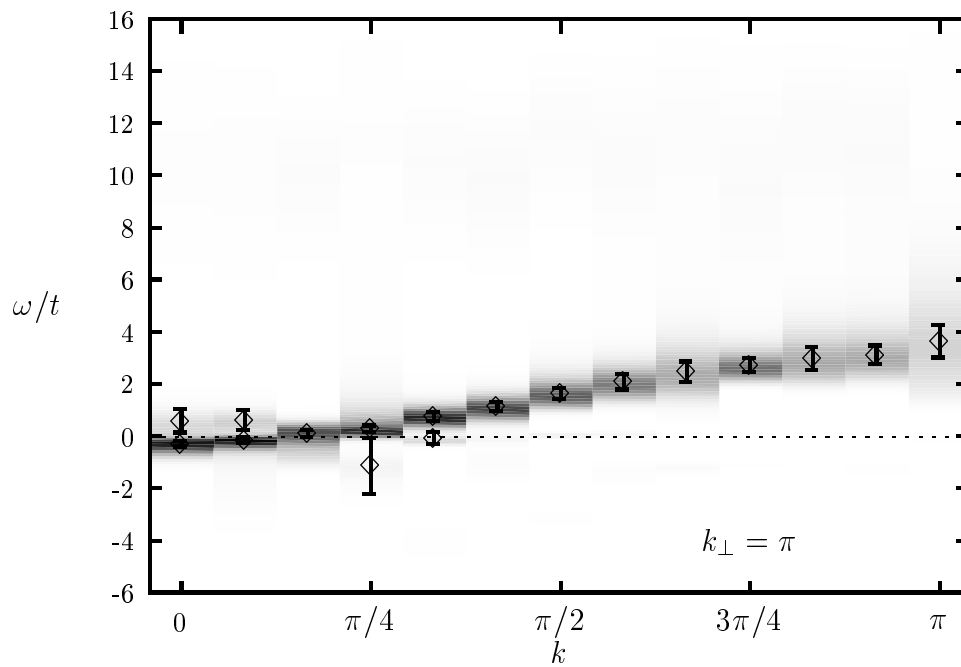
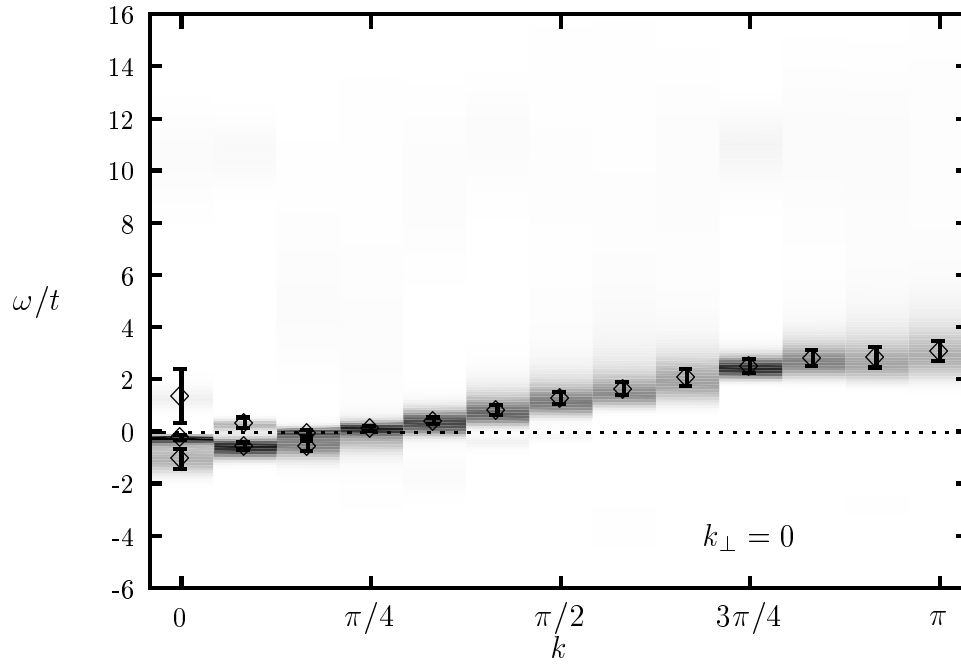
FIG. 1. QMC result for $A(\mathbf{k}, \omega)$ vs $\mathbf{k} = (k, k_{\perp})$ on a 2×24 Hubbard model with $U/t = 8$, $t_{\perp}/t = 0.15$ at $n = 1/3$ and an inverse temperature of $\beta t = 10$. Part (a) and (b) are density plots for the $k_{\perp} = 0$ and $k_{\perp} = \pi$ branches respectively with the darker shading corresponding to higher spectral weight, and the points with error bars showing the position of the peaks.

FIG. 2. Exact diagonalization result for the lowest excitation energies vs $\mathbf{k} = (k, k_{\perp})$ obtained on a 2×12 Hubbard model with $U/t = 8$, $t_{\perp}/t = 0.15$ at $n = 1/3$. The full symbols correspond to the main bonding and antibonding branches. Other low energy poles in $A_{\mathbf{k}, \omega}$ (with smaller spectral weight) are also indicated by open dots. The thin dotted lines correspond to the $U = 0$ case and the dashed line to the chemical potential.

FIG. 3. (a) Normalized splitting $\Delta E/2t_{\perp}$ extrapolated to $t_{\perp} \rightarrow 0$ (see text) vs U obtained by exact diagonalizations of 2×6 (open symbols) and 2×12 (full symbols) systems with on-site (O-S) Hubbard or intermediate range (I-R) repulsive interactions (see text). Both momenta $k > k_F$ (+) and $k < k_F$ (-) in the vicinity of k_F have been considered as indicated on the plot; (b) same quantity plotted as a function of α . The points with error bars correspond to crude estimates for the thermodynamic limit $N \rightarrow \infty$ (see text). Error bars are estimated from separate extrapolations of the (+) and (-) data.

FIG. 4. Spectral function $A(k, k_{\perp}, \omega)$ vs ω on a 2×12 system with $n = 1/3$ filling and for a longitudinal momentum $k = \pi/12 < k_F$. The full and dashed lines correspond to $k_{\perp} = \pi$ and $k_{\perp} = 0$, respectively. Only the $\omega < \mu$ region is shown (occupied states). (a) and (b) correspond to an on-site $U = 8$ Hubbard repulsion and to an intermediate range repulsion, $U = 6$, $V_1 = 3$ and $V_2 = 2$, respectively.

FIG. 5. Probability $P(\tau)$ for a 2×12 system at $n = 1/3$ filling and an extra hole with a longitudinal momentum $k = \pi/12 < k_F$. The dashed and full lines correspond to an on-site Hubbard repulsion $U = 8$ and to an intermediate range repulsion, with $U = 6$, $V_1 = 3$ and $V_2 = 2$, respectively.



2×24 -lattice, $U/t = 8$, $t_y/t = 0.15$,

$\beta t = 10$, $\langle n \rangle = 1/3$

$\Delta E/2t_y = 0.943 \pm 0.068$

